



# Effect of rolling temperature on microstructure and mechanical properties of 18%Mn TWIP/TRIP steels



Vladimir Torganchuk\*, Andrey Belyakov, Rustam Kaibyshev

Belgorod State University, Pobeda 85, Belgorod 308015, Russia

## ARTICLE INFO

### Keywords:

TWIP/TRIP steels  
Warm/hot rolling  
Recrystallization  
Mechanical properties

## ABSTRACT

The microstructure and mechanical properties of Fe-18Mn-0.6C and Fe-18Mn-0.4C steels subjected to rolling with a total reduction of 60% at temperatures of 773 K to 1373 K were investigated. Warm rolling at temperatures of 773–1073 K resulted in flattened grain structure with the transverse grain size of 7  $\mu\text{m}$ , whereas hot rolling at 1073–1373 K was accompanied by the dynamic recrystallization leading to almost equiaxed grains, the size of which increased with temperature. Internal stresses and corresponding dislocation densities increased as the rolling temperature decreased. The steel with higher carbon content exhibited finer grains and higher dislocation density after rolling. A decrease in the rolling temperature from 1373 K to 773 K resulted in a significant increase in the yield strength from about 300–400 MPa to 850–950 MPa, while ultimate tensile strength increased from 1000–1100 MPa to 1200–1300 MPa (the higher strength corresponds to higher carbon content). On the other hand, the total elongation decreased from approx. 85% in the Fe-18Mn-0.6C steel and from 65% in the Fe-18Mn-0.4C steel to approx. 30% in the both steels as the rolling temperature decreased from 1373 K to 773 K. The difference in the tensile behavior at room temperature was attributed to the variation in the deformation mechanisms. Namely, mechanical twinning operated in the both steels during tension, whereas  $\epsilon$ -martensite formation took place in the Fe-18Mn-0.4C steel.

## 1. Introduction

High-manganese austenitic steels exhibiting the effects of twinning-induced plasticity (TWIP) or/and transformation-induced plasticity (TRIP) are one of the most advanced materials used in the automobile industry [1]. The high-Mn TWIP/TRIP steels deform with a combination of dislocation glide and secondary deformation mechanisms such as the formation of  $\epsilon$ -martensite,  $\alpha'$ -martensite and/or mechanical twinning that provide a substantial strain hardening leading to outstanding plasticity [2–6]. The development of mechanical twinning or martensitic transformation in these steels depends on the stacking fault energy (SFE), which is in turn determined by alloying content and deformation temperature [7–10]. The most effective strain hardening has been reported for high-Mn TWIP steels with a SFE of  $\sim 25 \text{ mJ/m}^2$ . The proper value of SFE is usually achieved by alloying with Mn ( $\geq 18\%$ ), up to 0.6%C and to 6% of (Al + Si) [9,11–14]. Among those, the steels with reduced alloying content, i.e. those belonging Fe-18Mn-C system, have been attracting a remarkable interest among materials scientists and engineers for economic reasons. The total elongation up to 90% and the ultimate tensile strength of about 1000 MPa can be attained, although the yield strength is approx. 300 MPa in such steels

with recrystallized microstructure after conventional hot working or cold rolling followed by annealing [8,15–25]. Commonly, an increase in the carbon content was favorable for the yield strength, ultimate tensile strength, and ductility [20,26,27], although even 0.8%C did not result in significant changes of the strength and plastic properties, namely, the ultimate tensile strength and yield strength of about 1000 and 300 MPa, respectively, and a total elongation of 80% were reported for Fe-17Mn-0.6C hot rolled at 1273 K [28].

The strength level should generally depend on processing conditions including the rolling temperature. A decrease in the rolling temperature from 1373 K to 773 K resulted in remarkable strengthening of Fe-18Mn-(0.4–0.6)C steels [29]. Namely, the yield strengths increased from 300–360 MPa to 850–950 MPa, whereas the total elongations reduced from 70–80% to 30%, although the microstructure mechanisms responsible to the strengthening were not clarified [29]. The strengthening by warm-to-hot rolling is usually attributed to grain refinement (grain size strengthening) and work hardening (dislocation strengthening) [30–32]. Therefore, a modified Hall-Petch-type relationship incorporating the dislocation strengthening is frequently used to predict the yield strength of warm-to-hot worked steels [33–35]. However, the effect of temperature on the rolled microstructures and mechanical

\* Corresponding author.

E-mail address: [torganchuk@bsu.edu.ru](mailto:torganchuk@bsu.edu.ru) (V. Torganchuk).

properties of high-Mn TWIP/TRIP steels has not been studied in sufficient detail. The effect of processing conditions on the microstructure evolution and the development of dislocation substructures in high-Mn TWIP/TRIP steels during warm to hot rolling is still unclear.

The first aim of the present work is to study the effect of rolling temperature on the deformation microstructures and dislocation densities in Fe-18Mn-(0.4–0.6)C steels. The second aim is to reveal the relationship between the deformation structures/substructures and the mechanical properties of the warm to hot rolled steels with different SFE.

## 2. Materials and methods

Two high-Mn steels designated as Fe-18Mn-0.4C and Fe-18Mn-0.6C were examined. The actual chemical compositions were Fe-17.4Mn-0.44C-0.33Si-0.09Cr-0.01Al and Fe-18.0Mn-0.62C-0.24Si-0.04Cr-0.01Al (all in weight percent). The steels were produced by an induction melting and hot rolling at 1423 K with 60% reduction. The starting materials were characterized by uniform microstructures consisting of equiaxed grains with average sizes of 60  $\mu\text{m}$  and 50  $\mu\text{m}$  in Fe-18Mn-0.4C and Fe-18Mn-0.6C steels, respectively. The steels were subjected to plate rolling at various temperatures from 773 K to 1373 K to a total rolling reduction of 60%. After each rolling pass with about 10% reduction, the samples were re-heated to the designated rolling temperature.

The specimens were cut from the central parts of the rolled sheets with RD-ND sections for microhardness tests, microstructure observations and X-ray diffraction analysis (Fig. 1). The microstructural observations were carried out using a Jeol JEM 2100 transmission electron microscope (TEM) and a Quanta 600 scanning electron microscope (SEM) equipped with an electron back scattering diffraction pattern (EBSD) analyzer incorporating an orientation imaging microscopy (OIM) system. For the SEM observations and X-ray diffraction, the samples were electro-polished at a voltage of 20 V at room temperature using an electrolyte containing 10% perchloric acid and 90% acetic acid.

The OIM images were subjected to clean up procedure, i.e. the orientations with confidence index below 0.1 were replaced by their

confident neighbors (the number of replaced points did not exceed 10% for each OIM image). The high-angle boundaries were defined when the adjacent pixels in the orientation map had a misorientation of  $\geq 15^\circ$  and depicted in misorientation maps using black lines. The low-angle subboundaries with misorientations below  $15^\circ$  are not indicated in the OIM micrographs. The mean grain size was measured using the linear intercept method on the OIM images counting the distance between high-angle boundaries. The recrystallized fraction was evaluated as the area fraction of recrystallized grains (calculated by OIM Analysis 6.2).

The dislocation density was evaluated by X-ray diffraction profile analysis using an ARL-Xtra diffractometer operated at 45 kV and 35 mA with Cu K $\alpha$  radiation. The dislocation density was determined using the associated X-ray line broadening for {111} and {222} reflections. The X-ray line broadening was obtained using Lorentz function to approximate the spectrum as follows [36–39]:

$$\beta = B_m - B_i \quad (1)$$

where  $B_m$  is the measured full width at the half maximum height (FWHM) of K $\alpha$ 1 line and  $B_i$  is FWHM of an annealed silicon powder. The dislocation density ( $\rho$ ) was calculated from the average values of microstrain ( $\epsilon$ ) by the following relationship [40]:

$$\rho = 16.1\epsilon b^{-2} \quad (2)$$

where  $b$  is the Burgers vector, and the microstrains were evaluated by the Williamson-Hall method using the  $\beta$  values obtained by Eq. (1) [38,41].

For the TEM microstructure characterization after tensile tests, the thin foils of 3 mm in diameter were cut out parallel to RD-TD plane and ground to 0.1 mm in thickness. Then, the discs were polished using a double jet TENUPO-5 electrolytic polisher at voltage of 40 V at  $-30^\circ\text{C}$  with an electrolyte containing 5% perchloric acid and 95% ethanol. The tensile tests were performed along the rolling direction at ambient temperature at an initial strain rate of  $10^{-3}\text{ s}^{-1}$  using an INSTRON 5882.

The volume fractions of  $\alpha'$ -martensite/ferrite phase in the specimens after tensile tests were measured by the magnetic induction method using a Feritscope FMP30 (Fischer Technology, Inc., Windsor, CT). Before each measurement the sensor was calibrated against steel standards with 0.56%, 3.25%, 10.3%, 54.6% and 100% ferrite. The magnetic measurements were carried out near the fracture surface of tensioned specimens.

## 3. Results

### 3.1. Warm to hot rolled microstructures

Fig. 2 presents typical deformation microstructures of the warm to hot rolled steels. The warm rolling in the temperature interval of 773–973 K results in the development of pancake grain structure. Representative microstructures evolved at 873 K are shown for this temperature range in Figs. 2a and 2d. The deformation grains are flattened and highly elongated along the rolling direction. On the other hand, almost equiaxed grains evolve during the hot rolling at 1173–1373 K (representative microstructures evolved at 1373 K are shown for this temperature range in Figs. 2c and 2f). The grain structures developed during hot rolling involve a number of annealing twins. This suggests that the hot rolled microstructures resulted from discontinuous dynamic or post-dynamic recrystallization. At an intermediate temperature of 1073 K, partially recrystallized microstructures are developed, and the volume fraction of recrystallized grains strongly depends on the chemical composition of steels (cf. Figs. 2b and 2e). The deformation microstructure in the Fe-18Mn-0.6C consists almost completely of equiaxed fine grains. In contrast, the Fe-18Mn-0.4C steel processed by rolling at 1073 K is characterized by a necklace-like microstructure, where the original flattened grains are surrounded by chains of fine recrystallized ones [42]. The fraction of recrystallized grains does not exceed 0.4.

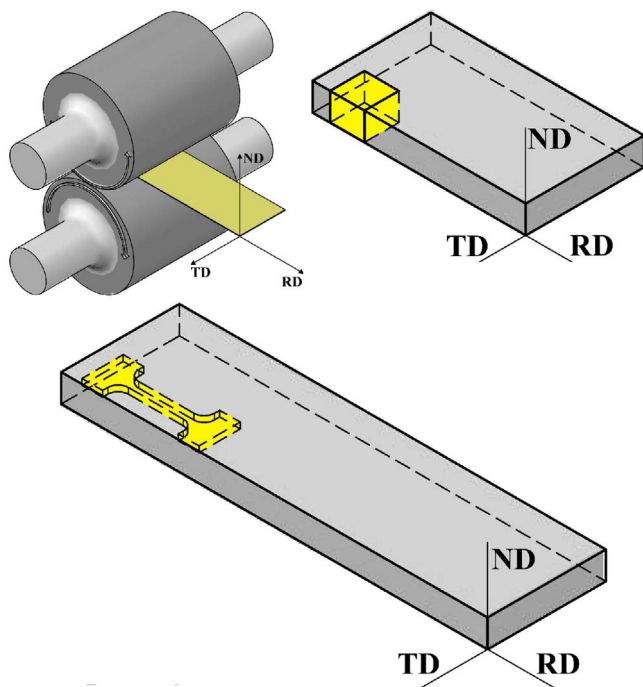


Fig. 1. Schematic representation of the sample sections for microstructural observations and tensile tests. RD, ND and TD are the rolling direction, normal direction and transverse direction, respectively.

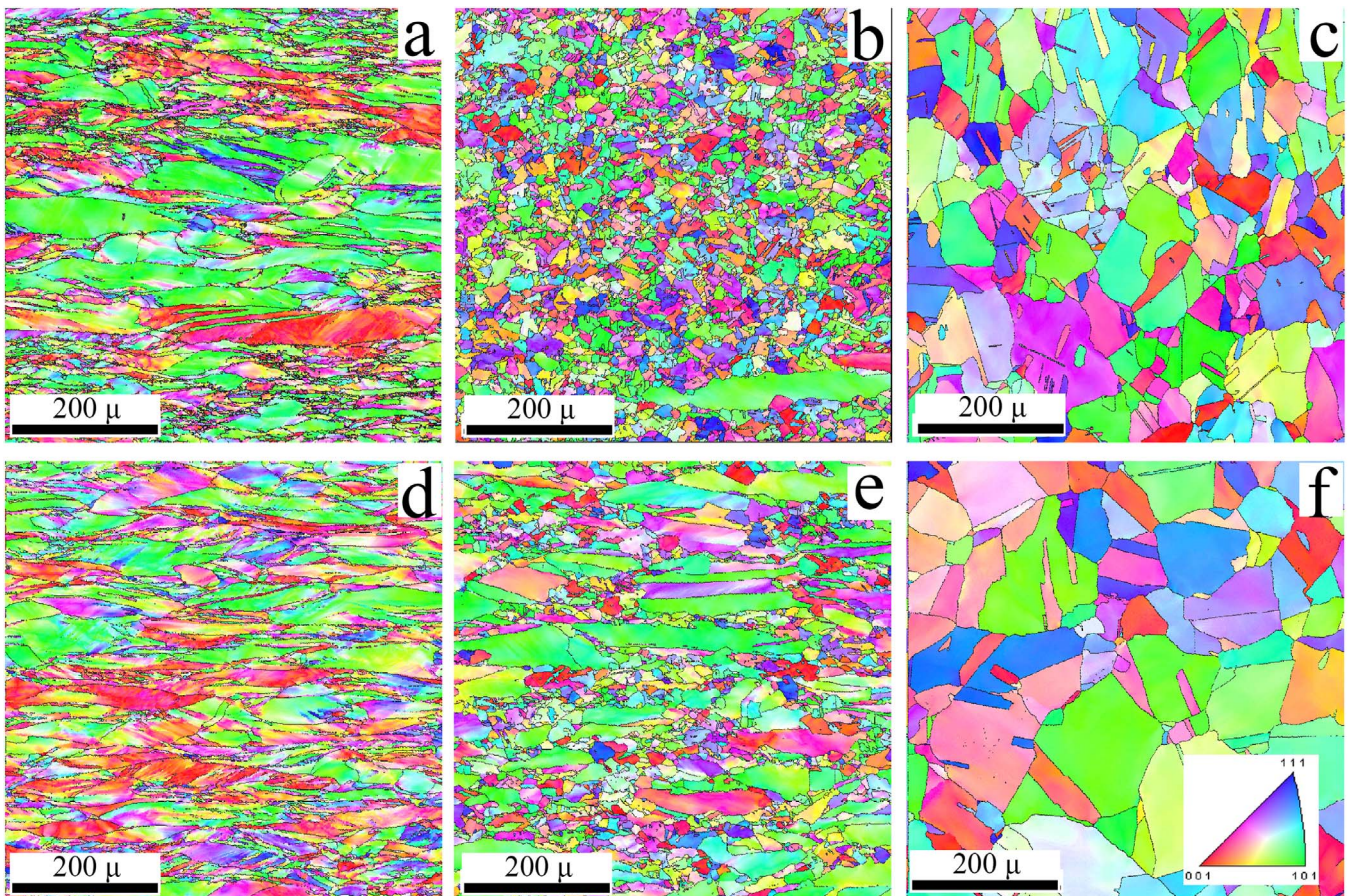


Fig. 2. Typical OIM images of microstructures in the Fe-18Mn-0.6C steel (a, b, c) and the Fe-18Mn-0.4C steel (d, e, f) after rolling at 873 K (a, d), 1073 K (b, e), and 1373 K (c, f). The colors correspond to the normal direction.

The transverse grain size for the Fe-18Mn-0.6C and Fe-18Mn-0.4C steels subjected to warm to hot rolling is shown in Fig. 3 as a function of the rolling temperature. The transverse grain size does not depend on the rolling temperature and is about 7  $\mu\text{m}$  in both steels processed by rolling at temperatures of 773–1073 K. This rolling temperature domain corresponds to warm deformation, when the original grains are flattened in accordance with rolling reduction, which predicts the transverse grain size of about 20  $\mu\text{m}$  (i.e., 60% reduction of 50–60  $\mu\text{m}$  initial grains). The smaller transverse grain size obtained by microstructural observations could result from the development of strain-induced grain boundaries. The grain subdivision by newly developed boundaries is frequently observed process during large strain deformations [33]. It is interesting to note that the number of strain-induced boundaries is the

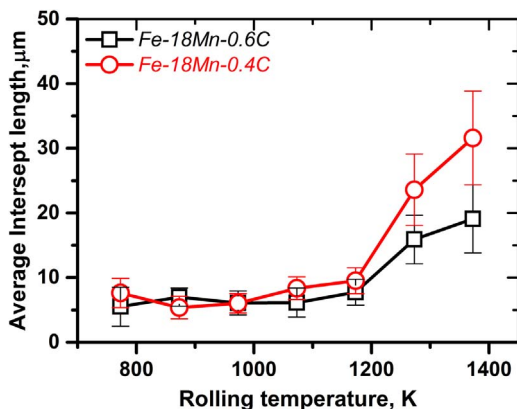


Fig. 3. Variations of the transverse grain size with the rolling temperature.

same in the both steels and does not vary with rolling temperature in the range of 773–973 K. In contrast, the transverse grain size evolved during hot rolling increases to 19  $\mu\text{m}$  and 32  $\mu\text{m}$  in the Fe-18Mn-0.6C and Fe-18Mn-0.4C steels, respectively, as the rolling temperature increases to 1373 K. Commonly, the recrystallized grain size depends on nucleation rate and growth rate [43]. An increase in the rolling temperature promotes the grain boundary mobility and suppresses the recrystallization nucleation because of a decrease in the deformation stored energy and, therefore, increases the recrystallized grain size. The Fe-18Mn-0.6C steel is characterized by finer grains as compared to Fe-18Mn-0.4C one after hot rolling that could be affected by a difference in the solute drag pressure retarding the grain growth [29].

The representative diffraction patterns for the steels subjected to rolling at different temperatures are shown in Fig. 4 and the effect of the rolling temperature on the dislocation density as revealed by X-ray analysis is shown in Fig. 5 (the lines in Fig. 5 represent the best fit by equations like  $\rho \sim k_1 \exp(k_2/T)$ , where  $k_1$  and  $k_2$  are constants, and  $T$  is the temperature). Commonly, the dislocation density decreases with an increase in the rolling temperature, and the Fe-18Mn-0.6C steel exhibits higher dislocation density than Fe-18Mn-0.4C one irrespective of the rolling temperature. It is worth noting that the deformation microstructure evolved during warm rolling is characterized by very high dislocation density, which is comparable with that observed in a similar TWIP steel after cold rolling [44]. The dislocation density rapidly decreases from  $3.6 \times 10^{15} \text{ m}^{-2}$  and  $2 \times 10^{15} \text{ m}^{-2}$  in the Fe-18Mn-0.6C and Fe-18Mn-0.4C steels, respectively, with an increase in the rolling temperature from 773 to 1073 K. Then, the rate of dislocation density change slows down in the hot rolling temperature domain, leading to dislocation density of  $2.2 \times 10^{14} \text{ m}^{-2}$  and  $7.9 \times 10^{13} \text{ m}^{-2}$  in the Fe-18Mn-0.6C and Fe-18Mn-0.4C steels, respectively, as the rolling

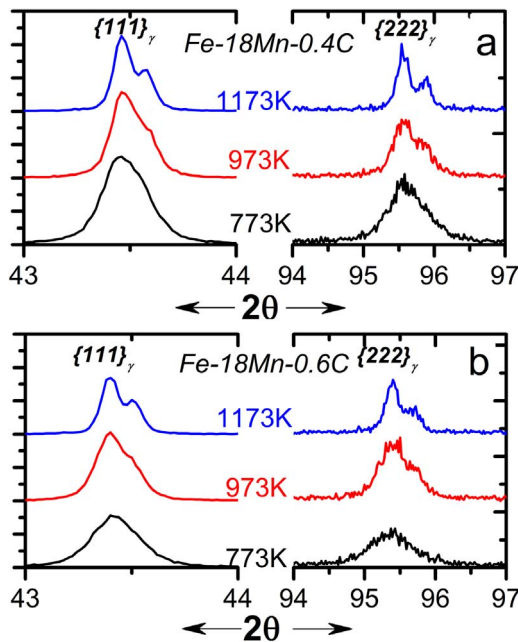


Fig. 4. XRD patterns for the Fe-18Mn-0.4C (a) and Fe-18Mn-0.6C (b) steels after hot/warm rolling at temperatures of 773 K, 973 K and 1173 K.

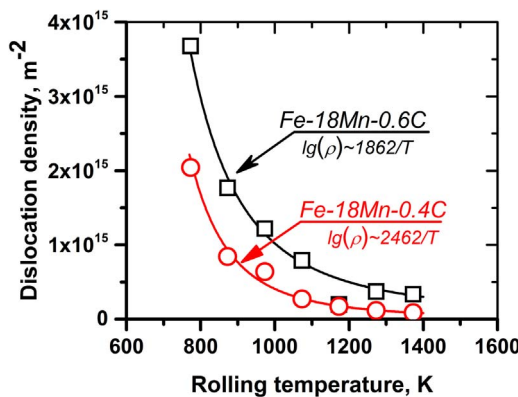


Fig. 5. Relationship between the rolling temperature and the dislocation density evolved in the Fe-18Mn-0.6C and Fe-18Mn-0.4C steels.

temperature increases to 1373 K. The high dislocation densities and their characteristic temperature dependencies suggest that static recrystallization scarcely affected the finally developed microstructures even after hot rolling. The microstructure evolution, therefore, results from dynamic recrystallization with a partial effect of post-dynamic recrystallization during the inter-pass re-heating period.

### 3.2. Tensile behavior

The true stress vs true strain curves for the Fe-18Mn-0.6C and Fe-18Mn-0.4C steels subjected to warm to hot rolling are shown in Fig. 6. The tensile tests show high levels of the maximal true stress, i.e., 1600–1900 MPa for Fe-18Mn-0.6C and 1500–1800 MPa for Fe-18Mn-0.4C. The flow curves of the samples rolled at 873–1373 K are characterized by serrations with amplitude increasing with straining that is typical feature of the deformation behavior of high-Mn austenitic steel alloyed with carbon [28,45]. A decrease of the rolling temperature results in a reduction in the number of serrations on the tensile curve (Fig. 6), although the frequency and amplitude of serrations depend also on the chemical composition of the steels. Both the frequency and amplitude increase with increasing the carbon content. After rolling at 773 K, any serrations on the tensile stress-strain curves can hardly be observed.

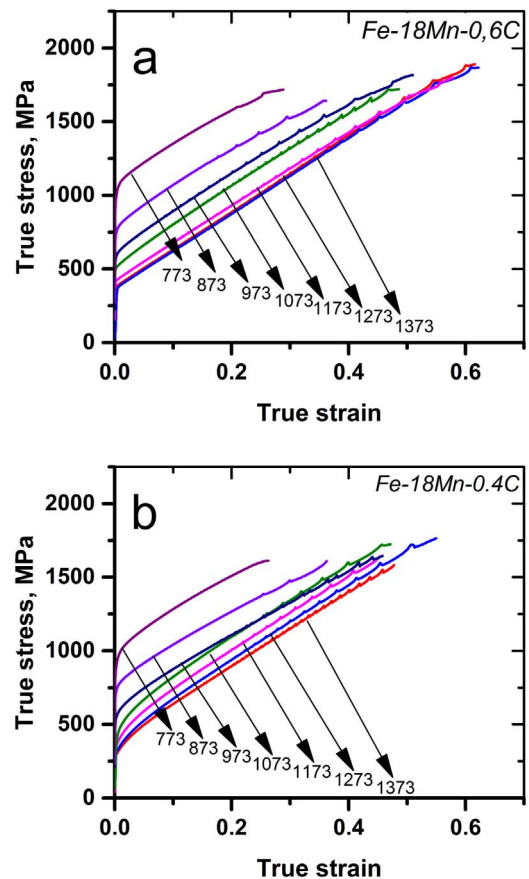


Fig. 6. True stress–strain curves obtained by tensile tests of the Fe-18Mn-0.6C (a) and Fe-18Mn-0.4C (b) steels processed by rolling at various indicated temperatures.

An increase in the rolling temperature from 773 K to 1373 K leads to a monotonic decrease in the yield strength from 950 MPa to 320 MPa and from 865 MPa to 255 MPa for the Fe-18Mn-0.6C and Fe-18Mn-0.4C steels, respectively (Fig. 7). On the other hand, the effect of rolling temperature on the ultimate tensile strength is much less pronounced. A decrease in the ultimate tensile strength with an increase in the rolling temperature is about 400 MPa for both steels. It is worth noting that the steels are characterized by quite different effect of the rolling temperature on the total elongation, although the temperature dependencies for the yield and tensile strength are similar in both steels. An increase in the rolling temperature leads to a monotonous increase of total elongation from about 30% to 80% in the Fe-18Mn-0.6C. In contrast, total elongation in the Fe-18Mn-0.4C steel increases from 30% to 65% with an increase in the rolling temperature from 773 K to 973 K and then does not change remarkably with further increase in the

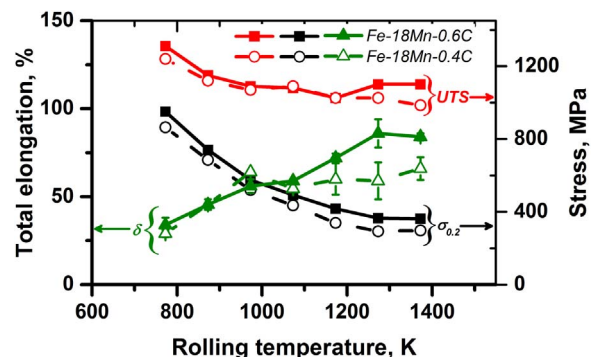
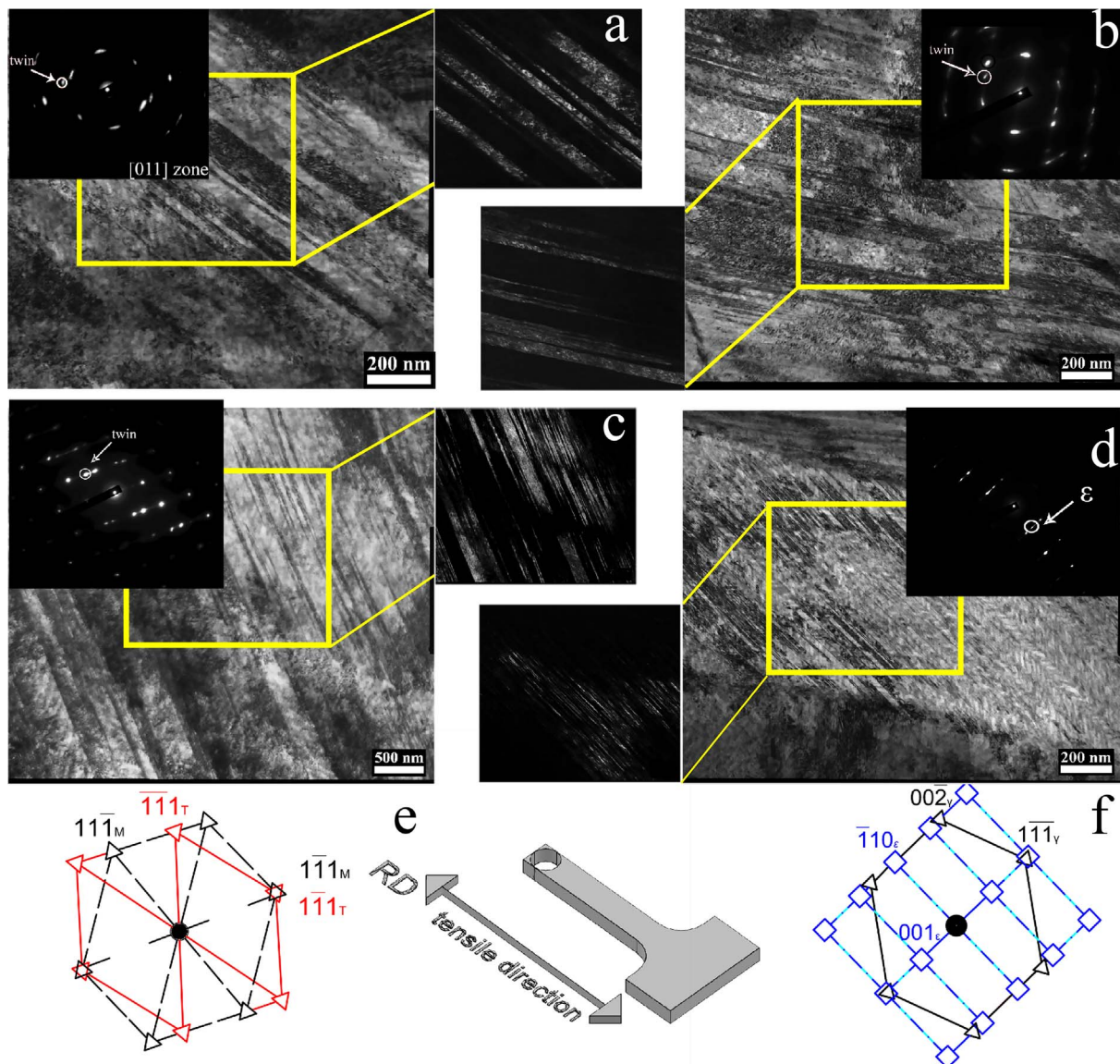


Fig. 7. Tensile behavior of the Fe-18Mn-0.6C and Fe-18Mn-0.4C steels processed by warm to hot rolling at temperatures of 773–1373 K.



**Fig. 8.** TEM images of microstructures after tensile tests at room temperature; (a) Fe-18Mn-0.6C processed by rolling at 1373 K, (b) Fe-18Mn-0.6C processed by rolling at 1073 K, (c) Fe-18Mn-0.6C processed by rolling at 773 K, (d) Fe-18Mn-0.4C processed by rolling at 1073 K, (e) and (f) are representations of diffraction patterns for twins and  $\epsilon$ -martensite in fcc crystals, respectively, along with a schematic clarification of the TEM specimen preparation.

temperature. It should be noted that the transition from warm to hot rolling is not accompanied by any sudden change in the temperature dependences of strength properties. In contrast, ductility of the Fe-18Mn-0.4C steel exhibits rather strong temperature dependence in the range of warm rolling and becomes apparently temperature invariant in the range of hot rolling (Fig. 7).

Fig. 8 shows several distinctive examples of microstructural changes caused by tensile tests of the Fe-18Mn-0.6C and Fe-18Mn-0.4C steels processed by warm to hot rolling. The samples for TEM observations were cut as close to the fracture surface of tensile specimens as possible. It is clearly seen in Figs. 8a to 8c that tensile tests of the Fe-18Mn-0.6C steel are assisted by the frequent deformation twinning, which results in the formation of nano-twinned microstructure consisting of numerous twins with an average transverse size well below 100 nm irrespective of the temperature of preceding rolling in the range of 773–1373 K. On the other hand, the  $\epsilon$ -martensite appears along with deformation twinning in the Fe-18Mn-0.4C steels during the tensile tests (Fig. 8d). The thickness of  $\epsilon$ -martensite plates does not exceed 20 nm and they are arranged parallel to deformation twins as evidenced by the diffraction pattern and dark field image in Fig. 8d.

Besides  $\epsilon$ -martensite, the present steels are also characterized by the different development of  $\alpha'$ -martensite after tensile tests (Fig. 9). The fraction of magnetic phase is almost zero (at the background level) in the Fe-18Mn-0.6C steel irrespective of the temperature of previous processing. In contrast, the Fe-18Mn-0.4C steel is characterized by a small amount of  $\alpha'$ -martensite, whose percentage increases from 1% to 5% as the rolling temperature increases from 773 K to 1373 K.

#### 4. Discussion

The microstructure evolution in the present steels during warm and hot rolling is typical for fcc metals with low to medium SFE [35,46]. The warm rolling leads to the elongation of original grains along the rolling axis and brings about a high dislocation density [29,30,47,48]. An increase in the rolling temperature promotes the development of discontinuous dynamic (and post-dynamic) recrystallization resulting in the new fine grains, the size and volume fraction of which depend on processing temperature. The fully recrystallized microstructure in the present steels is observed after hot rolling at temperatures above 1173 K. The formation of new grains in the Fe-18Mn-0.6C steel is

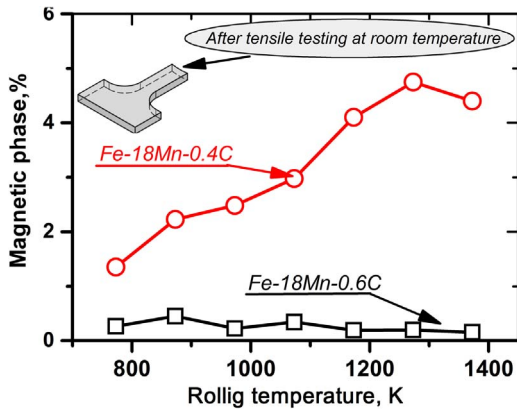


Fig. 9. Relationship between the magnetic phase and rolling temperature in the Fe-18Mn-0.6C and Fe-18Mn-0.4C steels after tensile tests.

observed at lower temperature than in the Fe-18Mn-0.4C steel. The number of fine grains in the rolled Fe-18Mn-0.6C steel at 1073 K, which is close to a critical recrystallization temperature, is much larger than that in the Fe-18Mn-0.4C steel. Increasing the rolling temperature leads to the formation of larger grains in accordance with general regularities of dynamic recrystallization, which predict the dynamic grain size ( $D$ ) being a power law function of flow stress ( $\sigma$ ), i.e.,  $(\sigma/G)(D/b)^{2/3} = K$ , where  $G$  is the shear modulus and  $K$  is a constant [32]. Correspondingly, the dislocation density, which can be related to the flow stress increment, i.e.  $\Delta\sigma \sim Gb\sqrt{\rho}$  [31,49], increases with a decrease in the rolling temperature. The average grain size is lower while the dislocation density is higher in the Fe-18Mn-0.6C steel than those in Fe-18Mn-0.4C steel. This behavior may be caused by different carbon content in these steels. The carbon provides an additional solution hardening and, therefore, increases the flow stress. The warm to hot working under higher flow stresses should be accompanied by the evolution of finer recrystallized grains with higher dislocation density. Moreover, an increase in the flow stress increases the stored energy and provides additional driving force for recrystallization nucleation.

The work hardening by warm to hot rolling is commonly related to an increase in the dislocation density [31,35]. Then, the yield strength of work hardened metallic materials can be expressed as follows: [31,43]:

$$\sigma_{0.2} = \sigma_0 + a M G b \sqrt{\rho} \quad (3)$$

where  $\sigma_0$  is the strength of the same material without dislocations,  $M$  is the Taylor factor and  $a$  is a constant. The first term in Eq. (3),  $\sigma_0$ , includes the Peierls stress of about 28 MPa for the present steels [50] and the solid solution strengthening [51]:

$$\Delta\sigma_{ss} = \sum K_i C_i^n \quad (4)$$

where  $K_{Mn} = 2.8 \text{ MPa wt}\%^{-1}$ ,  $K_C = 250 \text{ MPa wt}\%^{-1}$  and  $n = 2/3$  [51]. Thus,  $\sigma_0$  is about 190 MPa and 230 MPa for the Fe-18Mn-0.4 C and Fe-18Mn-0.6 C steels, respectively. Taking  $\alpha = 0.23$  [52], the dislocation densities can be calculated from Eq. (3). Fig. 10 presents the work hardening (dislocation strengthening) by rolling at various temperatures of the present steels and the relationship between the dislocation densities evaluated by X-ray diffraction (Eq. (2)) and work hardening (Eq. (3)). The direct linear relationships in Fig. 10b for the both steels testify to the speculations about the dislocation strengthening of the warm to hot worked steels above. The different slopes in Fig. 10b may result from effect of carbon content on the dislocation strengthening efficiency in the steels. The steel with smaller carbon content has lower SFE and, therefore, is less susceptible to dynamic recovery, which promotes the dislocation rearrangement and may diminish the efficiency of dislocation strengthening, although this interesting phenomenon should be further investigated in more detail.

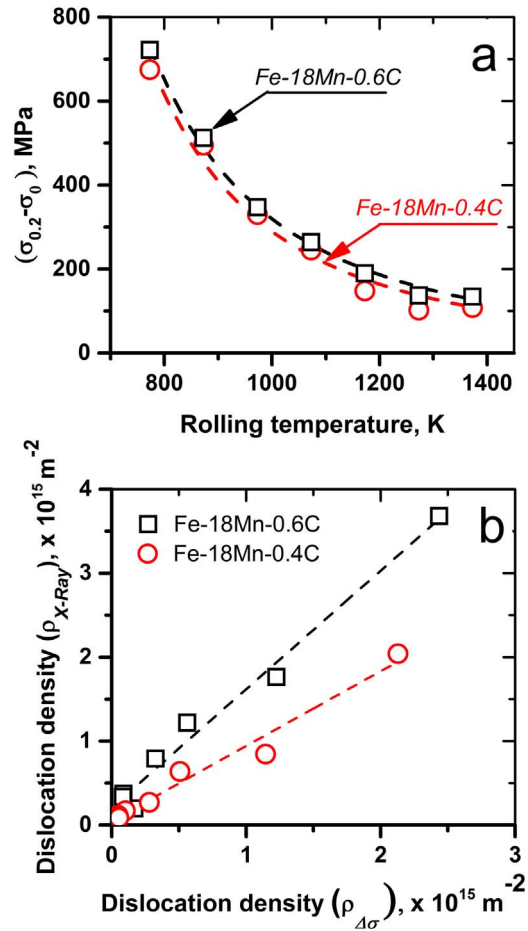


Fig. 10. Relationship between the rolling temperature and the dislocation strengthening for the Fe-18Mn-0.6C and Fe-18Mn-0.4C steels (a) and the comparison between the measured and calculated dislocation density.

Products of strength and total elongation are frequently used to compare the mechanical behavior of various structural steels and alloys in quantitative manner. The values of  $\sigma_{0.2} \times \delta$  and  $UTS \times \delta$  for the present steels processed by warm to hot rolling are represented in Fig. 11. It is clearly seen in Fig. 11 that the present steels are characterized by a quite different effect of the rolling temperature on their mechanical properties. The strengthening with a decrease in the rolling temperature is commonly accompanied by a degradation of ductility. Therefore, a decrease in the yield strength with increasing the temperature is compensated with an increase in the total elongation, and  $\sigma_{0.2} \times \delta$  slightly decreases in the range of 30–35 GPa % with an increase in the rolling temperature from 773 K to 1373 K for the Fe-18Mn-0.6C steel. The values of UTS for the present steels processed by warm to hot rolling do not depend on the magnitude of work hardening (Fig. 7) similar to other studies on high-Mn TRIP/TWIP steels subjected to conventional rolling [17,34,53,54]. Therefore, the product of  $UTS \times \delta$  progressively increases from 35 to 95 GPa % with an increase in the rolling temperature from 773 K to 1373 K. It is worth noting that the Fe-18Mn-0.6C steel processed by warm rolling exhibits very high value of the yield strength up to 950 MPa provided by high dislocation density of  $3.6 \times 10^{15} \text{ m}^{-2}$ , which is comparable to that of  $(3.5\text{--}4.5) \times 10^{15} \text{ m}^{-2}$  observed in other high-Mn steel after large strain cold rolling [44]. However, such high dislocation density above  $10^{15} \text{ m}^{-2}$  in the warm rolled steel does not lead to significant drop in ductility, which retains at rather high level of  $\delta > 30\%$  resulting in  $UTS \times \delta$  being about 45 GPa %.

In contrast to the Fe-18Mn-0.6C steel, the Fe-18Mn-0.4C one is characterized by a lower ductility. The total elongation in the Fe-18Mn-

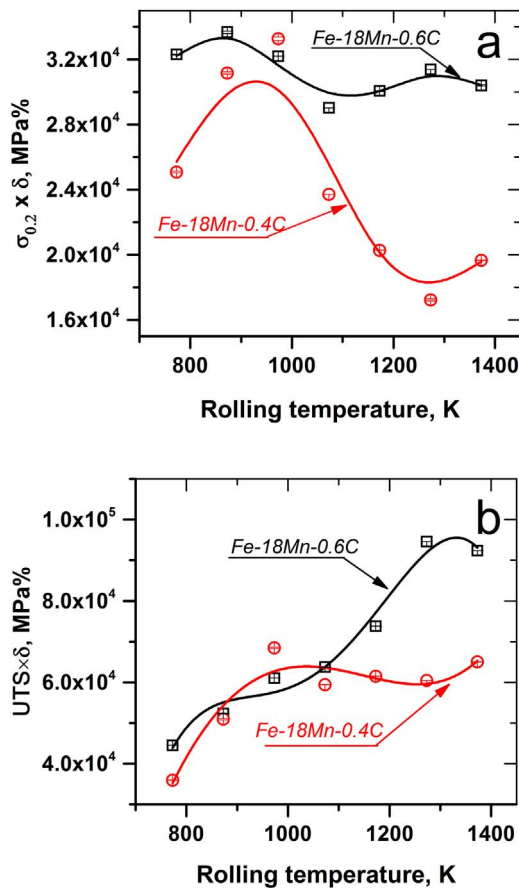


Fig. 11. Effect of the rolling temperature on the values of  $\sigma_{0.2} \times \delta$  and  $UTS \times \delta$  for Fe-18Mn-0.6C and Fe-18Mn-0.4C steels.

0.4C steel increases to about 65% with an increase in the rolling temperature to 973 K followed by an apparent saturation at a level of  $\delta \sim 60\%$  in spite of further increasing temperature (Fig. 7). Therefore, the product of  $\sigma_{0.2} \times \delta$  for the Fe-18Mn-0.4C steel increases to its maximum above 30 GPa % with increasing the rolling temperature to 973 K and, then, drastically decreases below 20 GPa % as the rolling temperature increases above 1173 K (Fig. 11). Correspondingly, following an increase with temperature in the range of 773–973 K, the product of  $UTS \times \delta$  for this steel tends to saturate at 60–70 GPa % with an increase in the rolling temperature above 1073 K.

The difference in the mechanical behavior between the Fe-18Mn-0.6C and Fe-18Mn-0.4C steels processed by warm to hot rolling is associated with the different deformation mechanisms operating during tensile testing. A decrease in the carbon content decreases SFE of high-Mn TWIP/TRIP steels [9]. Therefore, the Fe-18Mn-0.4C steel with lower SFE than Fe-18Mn-0.6C one is more susceptible to  $\epsilon$ -martensitic transformation during cold deformation (see Fig. 8). Moreover, the Fe-18Mn-0.4C steel is characterized by lower austenite stability than the Fe-18Mn-0.6C steel as proved by magnetic tests (Fig. 9). In general, the TWIP effect provides larger ductility than the TRIP effect [55,56]. In the present study the development of  $\epsilon$ -martensite during tensile tests of the Fe-18Mn-0.4C steel limits its ductility at a level of total elongation around 60–65%, whereas TWIP effect in the Fe-18Mn-0.6C steel provides total elongation above 80%. Nevertheless, both steels can be processed in a desirable strength-ductility combination by using warm to hot rolling at an appropriate rolling temperature.

## 5. Conclusions

The effect of rolling temperature ranging from 773 to 1373 K on the

microstructures and mechanical properties of Fe-18Mn-0.4C and Fe-18Mn-0.6C steels was investigated. The main results can be summarized as follows.

1. The warm rolling at temperatures of 773–973 K resulted in the evolution of pancake grain structures. In contrast, almost equiaxed grain structures (recrystallized microstructures) were developed during hot rolling at temperatures of 1173–1373 K. Rolling at 1073 K resulted in a partially recrystallized microstructure in the Fe-18Mn-0.4C steel, while almost fully recrystallized microstructure was observed in the Fe-18Mn-0.6C steel. The Fe-18Mn-0.6C steel was characterized by a smaller recrystallized grain size and a higher dislocation density as compared to Fe-18Mn-0.4C one.
2. A decrease in the rolling temperature resulted in remarkable strengthening, although plasticity degraded. An increase in the ultimate tensile strength with a decrease in the rolling temperature was less pronounced comparing to the yield strength. The Fe-18Mn-0.6C steel exhibited higher strength and larger ductility as compared to the Fe-18Mn-0.4C steel in the entire temperature range studied. An increase in the strength was attributed to work hardening (dislocation strengthening).
3. A product of the yield strength and total elongation ( $\sigma_{0.2} \times \delta$ ) for the Fe-18Mn-0.6C steel was above 30 GPa % within the studied temperature range, while that of ultimate tensile strength and total elongation ( $UTS \times \delta$ ) increased from 45 to 95 GPa % with an increase in the rolling temperature from 773 K to 1273 K. Such outstanding mechanical properties were provided by TWIP effect in the Fe-18Mn-0.6C steel. On the other hand,  $\sigma_{0.2} \times \delta$  for the Fe-18Mn-0.4C steel increased to a maximum of 33 GPa % with an increase in the rolling temperature to 973 K followed by a rapid drop below 20 GPa % as the rolling temperature increased above 1173 K. Correspondingly,  $UTS \times \delta$  for the Fe-18Mn-0.4C steel approached an apparent saturation of about 65 GPa % with increasing the rolling temperature to 973 K. This different effect of the rolling temperature on the tensile properties of the Fe-18Mn-0.4C and Fe-18Mn-0.6C steels was associated with  $\epsilon$ -martensitic transformation, which occurred in the Fe-18Mn-0.4C steel during the tensile tests and limited plasticity at a level of 65% total elongation after hot rolling.

## Acknowledgments

The financial support received from the Ministry of Education and Science, Russia, under Grant no. 11.3719.2017/PCh is gratefully acknowledged.

## References

- [1] B.C. De Cooman, K. Chin, J. Kim, High Mn TWIP Steels for Automotive Applications // New Trends and Developments In Automotive System Engineering, InTech, Rijeka, 2011.
- [2] A.S. Hamada, L.P. Karjalainen, M.C. Somani, The influence of aluminum on hot deformation behavior and tensile properties of high-Mn TWIP steels, Mater. Sci. Eng. A. 467 (2007) 114–124.
- [3] D.T. Pierce, J.A. Jiménez, J. Bentley, D. Raabe, J.E. Wittig, The influence of stacking fault energy on the microstructural and strain-hardening evolution of Fe–Mn–Al–Si steels during tensile deformation, Acta Mater. 100 (2015) 178–190.
- [4] L. Bracke, K. Verbeken, L. Kestens, J. Penning, Microstructure and texture evolution during cold rolling and annealing of a high Mn TWIP steel, Acta Mater. 57 (2009) 1512–1524.
- [5] S. Vercammen, B. Blanpain, B.C. De Cooman, P. Wollants, Cold rolling behaviour of an austenitic Fe–30Mn–3Al–3Si TWIP-steel: the importance of deformation twinning, Acta Mater. 52 (2004) 2005–2012.
- [6] O. Grässel, L. Krüger, G. Frommeyer, L.W. Meyer, High strength Fe–Mn–(Al, Si) TRIP/TWIP steels development—properties—application, Int. J. Plast. 16 (2000) 1391–1409.
- [7] D. Rafaja, C. Krbetschek, C. Ullrich, S. Martin, Stacking fault energy in austenitic steels determined by using *in situ* X-ray diffraction during bending, J. Appl. Crystallogr. 47 (2014) 936–947.
- [8] J.-K. Kim, B.C. De Cooman, Stacking fault energy and deformation mechanisms in Fe-xMn-0.6C-yAl TWIP steel, Mater. Sci. Eng. A. 676 (2016) 216–231.
- [9] A. Saeed-Akbari, L. Mosecker, A. Schwedt, W. Bleck, Characterization and

- prediction of flow behavior in high-manganese twinning induced plasticity steels: Part I. Mechanism maps and work-hardening behavior, *Metall. Mater. Trans. A*. 43 (2012) 1688–1704.
- [10] L. Rémy, A. Pineau, B. Thomas, Temperature dependence of stacking fault energy in close-packed metals and alloys, *Mater. Sci. Eng.* 36 (1978) 47–63.
- [11] J. Kim, S.-J. Lee, B.C. De Cooman, Effect of Al on the stacking fault energy of Fe–18Mn–0.6C twinning-induced plasticity, *Scr. Mater.* 65 (2011) 363–366.
- [12] J. Yoo, K. Han, Y. Park, C. Lee, Effect of silicon on the solidification cracking behavior and metastable carbide formation in austenitic high Mn steel welds, *Mater. Chem. Phys.* 148 (2014) 499–502.
- [13] R. Xiong, H. Peng, S. Wang, H. Si, Y. Wen, Effect of stacking fault energy on work hardening behaviors in Fe–Mn–Si–C high manganese steels by varying silicon and carbon contents, *Mater. Des.* 85 (2015) 707–714.
- [14] K.-T. Park, K.G. Jin, S.H. Han, S.W. Hwang, K. Choi, C.S. Lee, Stacking fault energy and plastic deformation of fully austenitic high manganese steels: Effect of Al addition, *Mater. Sci. Eng. A*. 527 (2010) 3651–3661.
- [15] M.I. Latypov, S. Shin, B.C. De Cooman, H.S. Kim, Micromechanical finite element analysis of strain partitioning in multiphase medium manganese TWIP + TRIP steel, *Acta Mater.* 108 (2016) 219–228.
- [16] Z. Yanushkevich, A. Belyakov, R. Kaibyshev, C. Haase, D.A. Molodov, Effect of cold rolling on recrystallization and tensile behavior of a high-Mn steel, *Mater. Charact.* 112 (2016) 180–187.
- [17] D. Pérez Escobar, S. Silva Ferreira de Dafé, K. Verbeke, D. Brandão Santos, Effect of the Cold Rolling Reduction on the Microstructural Characteristics and Mechanical Behavior of a 0.06% C–17% Mn TRIP/TWIP Steel, *Steel Res. Int.* 87 (2016) 95–106.
- [18] S.-M. Lee, I.-J. Park, J.-G. Jung, Y.-K. Lee, The effect of Si on hydrogen embrittlement of Fe–18Mn–0.6C–xSi twinning-induced plasticity steels, *Acta Mater.* 103 (2016) 264–272.
- [19] S. Kang, J.-G. Jung, M. Kang, W. Woo, Y.-K. Lee, The effects of grain size on yielding, strain hardening, and mechanical twinning in Fe–18Mn–0.6C–1.5Al twinning-induced plasticity steel, *Mater. Sci. Eng. A*. 652 (2016) 212–220.
- [20] H. Ding, D. Han, J. Zhang, Z. Cai, Z. Wu, M. Cai, Tensile deformation behavior analysis of low density Fe–18Mn–10Al–xC steels, *Mater. Sci. Eng. A*. 652 (2016) 69–76.
- [21] A.A. Gazder, A.A. Saleh, M.J.B. Nancarrow, D.R.G. Mitchell, E.V. Pereloma, A transmission kikuchi diffraction study of a cold-rolled and annealed Fe–17Mn–2Si–3Al–1Ni–0.06C wt% steel, *Steel Res. Int.* 86 (2015) 1204–1214.
- [22] P. Dastranjy Nezhadfar, A. Rezaeian, M. Sojudi Pakiadeh, Softening behavior of a cold rolled high-mn twinning-induced plasticity steel, *J. Mater. Eng. Perform.* 24 (2015) 3820–3825.
- [23] L. Chen, H.-S. Kim, S.-K. Kim, B.C. De Cooman, Localized deformation due to Portevin-LeChatelier effect in 18Mn–0.6C TWIP austenitic steel, *ISIJ Int.* 47 (2007) 1804–1812.
- [24] J.-E. Jin, Y.-K. Lee, Effects of Al on microstructure and tensile properties of C-bearing high Mn TWIP steel, *Acta Mater.* 60 (2012) 1680–1688.
- [25] M. Koyama, T. Sawaguchi, K. Tsuzaki, Deformation twinning behavior of twinning-induced plasticity steels with different carbon concentrations – Part 2: proposal of dynamic-strain-aging-assisted deformation twinning, *ISIJ Int.* 55 (2015) 1754–1761.
- [26] C.W. Shao, P. Zhang, R. Liu, Z.J. Zhang, J.C. Pang, Z.F. Zhang, Low-cycle and extremely-low-cycle fatigue behaviors of high-Mn austenitic TRIP/TWIP alloys: Property evaluation, damage mechanisms and life prediction, *Acta Mater.* 103 (2016) 781–795.
- [27] O. Bouaziz, S. Allain, C.P. Scott, P. Cugy, D. Barbier, High manganese austenitic twinning induced plasticity steels: a review of the microstructure properties relationships, *Curr. Opin. Solid State Mater. Sci.* 15 (2011) 141–168.
- [28] M. Koyama, T. Sawaguchi, T. Lee, C.S. Lee, K. Tsuzaki, Work hardening associated with  $\epsilon$ -martensitic transformation, deformation twinning and dynamic strain aging in Fe–17Mn–0.6C and Fe–17Mn–0.8C TWIP steels, *Mater. Sci. Eng. A*. 528 (2011) 7310–7316.
- [29] A. Belyakov, R. Kaibyshev, V. Torganchuk, Microstructure and Mechanical Properties of 18%Mn TWIP/TRIP steels processed by warm or hot rolling, *Steel Res. Int.* 88 (2017) 171–175.
- [30] Z. Yanushkevich, A. Belyakov, R. Kaibyshev, Microstructural evolution of a 304-type austenitic stainless steel during rolling at temperatures of 773–1273K, *Acta Mater.* 82 (2015) 244–254.
- [31] D. Hull, D.J. Bacon, *Introduction to Dislocations*, Pergamon, Oxford, 2001.
- [32] B. Derby, The dependence of grain size on stress during dynamic recrystallisation, *Acta Metall. Mater.* 39 (1991) 955–962.
- [33] D.A. Hughes, N. Hansen, Microstructure and strength of nickel at large strains, *Acta Mater.* 48 (2000) 2985–3004.
- [34] P. Kusakin, K. Tsuzaki, D.A. Molodov, R. Kaibyshev, A. Belyakov, Advanced thermomechanical processing for a high-Mn austenitic steel, *Metall. Mater. Trans. A*. 47A (2016) 5704–5708.
- [35] Z. Yanushkevich, A. Mogucheva, M. Tikhonova, A. Belyakov, R. Kaibyshev, Structural strengthening of an austenitic stainless steel subjected to warm-to-hot working, *Mater. Charact.* 62 (2011) 432–437.
- [36] B. Zhang, V.P.W. Shim, Effect of strain rate on microstructure of polycrystalline oxygen-free high conductivity copper severely deformed at liquid nitrogen temperature, *Acta Mater.* 58 (2010) 6810–6827.
- [37] T. Shintani, Y. Murata, Evaluation of the dislocation density and dislocation character in cold rolled Type 304 steel determined by profile analysis of X-ray diffraction, *Acta Mater.* 59 (2011) 4314–4322.
- [38] R.E. Smallman, K.H. Westmacott, Stacking faults in face-centred cubic metals and alloys, *Philos. Mag.* 2 (1957) 669–683.
- [39] Y.H. Zhao, K. Zhang, K. Lu, Structure characteristics of nanocrystalline element selenium with different grain sizes, *Phys. Rev. B*. 56 (1997) 14322.
- [40] G. Williamson, R. Smallman, III, Dislocation densities in some annealed and cold-worked metals from measurements on the X-ray debye-scherrer spectrum, *Philos. Mag.* 1 (1956) 34–46.
- [41] G. Williamson, W. Hall, X-ray line broadening from filed aluminium and wolfram, *Acta Metall.* 1 (1953) 22–31.
- [42] T. Sakai, A. Belyakov, R. Kaibyshev, H. Miura, J.J. Jonas, Dynamic and post-dynamic recrystallization under hot, cold and severe plastic deformation conditions, *Prog. Mater. Sci.* 60 (2014) 130–207.
- [43] A. Rollett, F. Humphreys, G.S. Rohrer, M. Hatherly, *Recrystallization and Related Annealing Phenomena*, Elsevier, Oxford, 2004.
- [44] P. Kusakin, A. Belyakov, C. Haase, R. Kaibyshev, D.A. Molodov, Microstructure evolution and strengthening mechanisms of Fe–23Mn–0.3C–1.5Al TWIP steel during cold rolling, *Mater. Sci. Eng. A*. 617 (2014) 52–60.
- [45] K. Jeong, J.-E. Jin, Y.-S. Jung, S. Kang, Y.-K. Lee, The effects of Si on the mechanical twinning and strain hardening of Fe–18Mn–0.6C twinning-induced plasticity steel, *Acta Mater.* 61 (2013) 3399–3410.
- [46] T. Lee, M. Koyama, K. Tsuzaki, Y.-H. Lee, C.S. Lee, Tensile deformation behavior of Fe–Mn–C TWIP steel with ultrafine elongated grain structure, *Mater. Lett.* 75 (2012) 169–171.
- [47] R. Song, D. Ponge, D. Raabe, R. Kaspar, Microstructure and crystallographic texture of an ultrafine grained C–Mn steel and their evolution during warm deformation and annealing, *Acta Mater.* 53 (2005) 845–858.
- [48] M.R. Barnett, J.J. Jonas, Distinctive aspects of the physical metallurgy of warm rolling, *ISIJ Int.* 39 (1999) 856–873.
- [49] E. Nes, Modelling of work hardening and stress saturation in FCC metals, *Prog. Mater. Sci.* 41 (1997) 129–193.
- [50] H.J. Frost, M.F. Ashby, *Deformation mechanism maps: the plasticity and creep of metals and ceramics*, Pergamon Press, Oxford, 1982.
- [51] P. Kusakin, A. Belyakov, D.A. Molodov, R. Kaibyshev, On the effect of chemical composition on yield strength of TWIP steels, *Mater. Sci. Eng. A*. 687 (2017) 82–84.
- [52] Z. Yanushkevich, A. Belyakov, C. Haase, D.A. Molodov, R. Kaibyshev, Structural/textural changes and strengthening of an advanced high-Mn steel subjected to cold rolling, *Mater. Sci. Eng. A*. 651 (2016) 763–773.
- [53] A.R. Khalesian, A. Zarei-Hanzaki, H.R. Abedi, F. Pilehva, An investigation into the room temperature mechanical properties and microstructural evolution of thermomechanically processed TWIP steel, *Mater. Sci. Eng. A*. 596 (2014) 200–206.
- [54] S. Lee, B.C. De Cooman, Annealing Temperature dependence of the tensile behavior of 10 pct Mn multi-phase TWIP-TRIP Steel, *Metall. Mater. Trans. A*. 45 (2014) 6039–6052.
- [55] D. Hua, T. Zheng-You, L. Wei, W. Mei, S. Dan, Microstructures and mechanical properties of Fe–Mn–(Al, Si) TRIP/TWIP steels, *J. Iron Steel Res. Int.* 13 (2006) 66–70.
- [56] G. Frommeyer, U. Brück, P. Neumann, Supra-ductile and high-strength manganese-TRIP/TWIP steels for high energy absorption purposes, *ISIJ Int.* 43 (2003) 438–446.